

# Plasmonic Fano resonances in compositional heterogenous Al-Au nanorod dimers

**Botao Wu, Yingxian Xue, Qiang Ma, Chengjie Ding, Youying Rong, Yan Liu, Lingxiao Chen, E Wu and Heping Zeng**

State Key Laboratory of Precision Spectroscopy, East China Normal University, Shanghai, 200062, China

E-mail: [btwu@phy.ecnu.edu.cn](mailto:btwu@phy.ecnu.edu.cn)

**Abstract.** We have investigated theoretically the plasmon resonance coupling in compositional heterogenous Al-Au nanorod dimers organized in a close proximity by end-to-end. It has been proved that the destructive interference between the bright dipole mode from Al nanorod and the dark quadrupole mode from Au nanorod nearby results in the appearance of apparent Fano resonance in the extinction spectra. The Fano resonance response on the structural dimension modifications in the proposed nanorod dimers have been estimated and determined. The Al-Au heterogeneous nanorod dimer shows a high sensitivity to the surrounding environment with a local surface plasmon resonance figure of merit of 7.6, which enables its promising applications in plasmonic sensing and detection.

## 1. Introduction

The unique optical properties of noble metal nanostructures because of the collective oscillations of free electrons on metal surface when coupled with light have attracted tremendous interest due to their ability to confine and manipulate electromagnetic waves beyond the diffraction limit and to tailor light-matter interactions down to nanometer scale, and thus have found a rich variety of fundamental techniques and applications in plasmonic photovoltaic cells,<sup>1</sup> surface-plasmon enhanced spectroscopies,<sup>2-6</sup> photochemistry and photocatalysis,<sup>7,8</sup> sensing,<sup>9</sup> and quantum optics.<sup>10-12</sup> The plasmonic properties of a metal nanostructure are closely related to its composition, shape, size, and the surrounding environment. When two or more metal nanostructures are placed closely, their individual plasmon modes will be coupled strongly by near-field interactions and produce hybridized plasmon modes.<sup>13,14</sup> Plasmon hybridization of complex metal nanostructures can induce extremely strong localized near field enhancement around the junctions between adjacent nanostructures, and enables applications in surface enhanced spectroscopies,<sup>2,4</sup> sensing,<sup>9</sup> and plasmonic rules.<sup>15</sup>

Plasmonic Fano resonance, originating from the interference between spectrally overlapping broad super-radiant bright and narrow sub-radiant dark plasmonic modes, is a unique consequence of near-field coupling in complex metal nanostructures. Fano resonance has been investigated in various plasmonic nanostructures formed by the same metal, including nanoparticle aggregates,<sup>16,17</sup> metal dimers,<sup>18</sup> ring/disk cavities,<sup>19</sup> metallic core-shell nanostructures.<sup>20</sup> Fano resonance has also been reported to a lesser extent in compositional heterogenous metal nanostructures, theoretically and experimentally.<sup>21-24</sup> Due to its narrow lineshape and high sensitivity to environmental media,



plasmonic Fano resonance shows potential applications in surface enhanced Raman scattering<sup>17</sup> and plasmonic biosensing.<sup>19</sup>

In this paper, we explored theoretically the optical properties of a new heterogeneous metal dimers composed of an aluminum (Al) and a gold (Au) nanorod. As shown in Fig. 1(a), the Al and Au nanorods are arranged by end-to-end with a small gap in between. Recently, Al nanorods have been reported to exhibit highly tunable plasmonic resonances from the deep ultraviolet to the visible wavelength region.<sup>25,26</sup> Here, the short Al nanorod supports a broad bright mode while the long Au nanorod supports a narrow dark mode. The interaction between them induces an apparent Fano dip in the extinction spectra of Al-Au nanorod dimers. The Fano resonance can be tuned by changing the Al or Au nanorod length and spatial separation in between, and shows a high sensitivity to the surrounding environment.

## 2. Computation methods

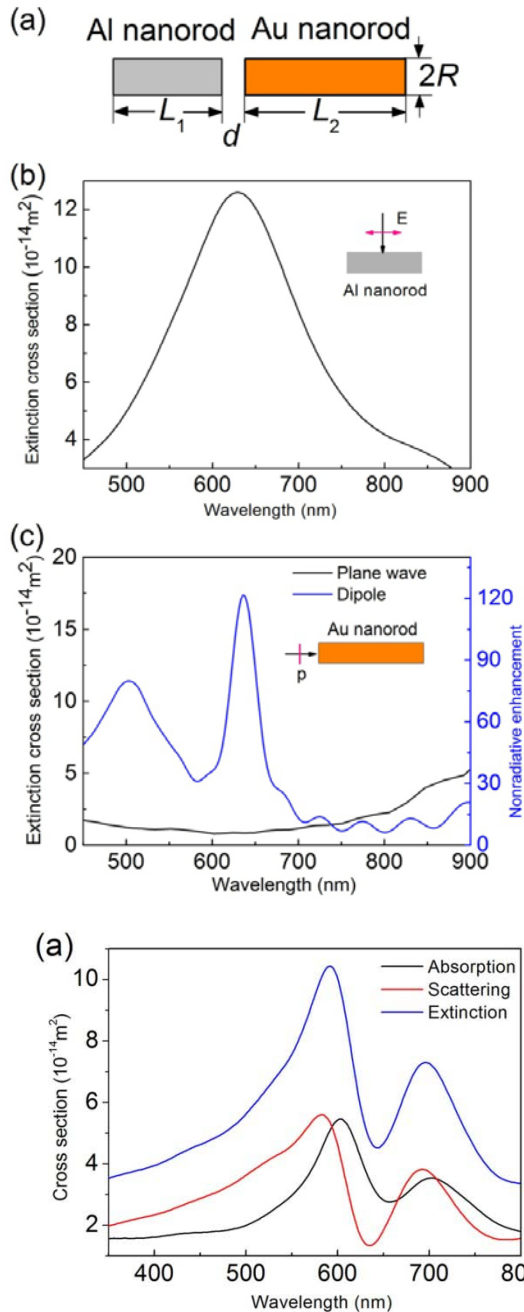
The numerical simulations were performed by the finite difference time domain (FDTD) Solutions software (Version 8.5, Lumerical Solution, Inc. Canada). The dielectric constants of aluminum and gold are taken from Ref. 27. The schematic geometry of Al-Au nanorod dimer is shown in Fig. 1(a). The Al and Au nanorods are coaxially arranged with the lengths of  $L_1$  and  $L_2$ , respectively and the diameter  $2R$ . The gap between the two nanorods is  $d$ . The refractive index of the surrounding matrix is set to be 1. A plane wave total field-scattered field source ranging from 200 to 900 nm is utilized as the incident light beam with linear polarization direction along the longitudinal axis of the nanorod dimer shown as  $x$  direction in Fig. 1(a). A three-dimensional nonuniform meshing is used, and a grid size of 0.5 nm is chosen for the inside and immediate vicinity of Al-Au nanorod dimers. We use perfectly matched layer absorption boundary conditions as well as symmetric boundary conditions to reduce the memory requirement and computational time. All the numerical results have been after prior convergence testing.

## 3. Results and discussion

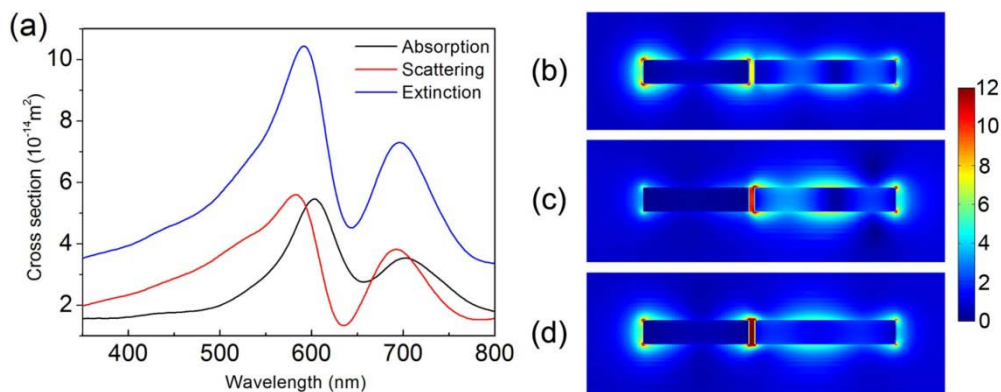
Firstly the bright and dark modes supported by single Al and Au nanorods are characterized and discussed. Fig. 1(b) presents the extinction spectrum of one single Al nanorod with the length  $L_1 = 187$  nm and the diameter  $2R = 40$  nm. A dipole plasmonic resonance peak around 630 nm is observed, and serves as a bright mode in Al-Au nanorod dimers. Meanwhile, although the dark mode has a weak coupling with the plane wave, it can be excited by a point source.<sup>28</sup> Fig. 1(c) exhibits the nonradiative enhancement of one single Au nanorod excited by a dipole source as well as its extinction spectrum illuminated by the normal plane wave. The diameter  $2R$  of Au nanorod is also 40 nm and its length  $L_2$  is 200 nm. The dipole source is placed along the longitudinal axis of Au nanorod with a gap distance  $d = 10$  nm from one end of the nanorod and its polarization is also along the longitudinal axis of the nanorod, as shown in the inset schematic of Fig. 1(c). It is seen that there is a resonance peak around 635 nm excited by the dipole source, but it cannot be excited by the normal plane wave, since it is a quadrupole plasmon resonance and can serve as a dark mode. Obviously, if the dipole source is replaced by the Al nanorod the dark mode in the Au nanorod will be excited when illuminated by the plane wave, and concomitantly Fano resonance will appear due to their good spectral overlapping.

Fig. 2(a) shows the extinction, scattering and absorption spectra of Al-Au heterogenous nanorod dimer consisting of the above mentioned Al and Au nanorods with  $d = 10$  nm. Clearly, a dip at 643 nm appears in the extinction spectrum. Actually the dip is induced by Fano interference. According to Ref. 14, when the dimer is illuminated at the frequencies resonating with both bright and dark modes, the bright mode of Al nanorod will be excited by two pathways:  $|I\rangle \rightarrow |B\rangle$  and  $|I\rangle \rightarrow |B\rangle \rightarrow |D\rangle \rightarrow |B\rangle$ , where  $|I\rangle$ ,  $|B\rangle$  and  $|D\rangle$  are excitation source, bright mode and dark mode, respectively. Fano-like interference occurs when the cumulative phase shift from  $|B\rangle \rightarrow |D\rangle \rightarrow |B\rangle$  is  $\pi$  so that the two pathways interfere destructively, canceling the polarization of the bright mode and resulting in a narrow Fano dip in the extinction spectrum as shown in Fig. 2(a). Simultaneously, the dipole and

quadrupole plasmon modes supported by the short Al and long Au nanorods hybridize in a constructive way to form two collective resonant modes: a high-energy antibonding mode at 592 nm and a low-energy bonding mode at 696 nm. The electric field distributions of the dimer with the separation  $d = 10$  nm at the wavelength of 592, 643 and 696 nm are shown in Fig. 2(b)-(d). The electric field enhancement of the bright mode Al nanorod at the Fano dip is greatly depressed due to the cancelation of its polarization in the Fano resonance (see Fig. 2c).



**Figure 1.** (a) Geometry of Al-Au heterogenous nanorod dimer; (b) Extinction spectrum of a short Al nanorod with  $L_1 = 187$  nm and  $2R = 40$  nm. The inset shows the schematic of the nanorod illuminated by a plane wave; (c) Extinction spectrum (black curve) and nonradiative enhancement (blue curve) of a long Au nanorod with  $L_2 = 250$  nm and  $2R = 40$  nm. The inset shows the configuration of the dipole-nanorod coupling system.



**Figure 2.** (a) Extinction, absorption and scattering spectra of Al-Au nanorod dimer with  $L_1 = 187$  nm,  $L_2 = 250$  nm, and  $2R = 40$  nm; Electric field distributions across the central cross section of the Al-Au nanorod dimer at (b)  $\lambda = 592$  nm; (c) 643 nm and (d) 696 nm.

As shown in Fig. 3, the Fano resonance characteristics in Al-Au nanorod dimer can be tuned by modulating the gap distance between the two nanorods. Decreasing the separation between the two nanorods enhances the coupling strength between the bright and dark modes, and concomitantly the Fano dip becomes deeper.<sup>28</sup> The deeper Fano dip may be useful in the application of sensing and plasmon induced transparency. In addition, the change of plasmon coupling strength shows more apparent effect on the low-energy peak ( $\lambda = 696$  nm) than that on the high-energy one ( $\lambda = 592$  nm). With the gap  $d$  increasing from 10 to 30 nm, the low-energy peak shows a blue shift of about 27 nm (from 696 to 669 nm), whereas the high-energy peak shows a red shift of about 7 nm (from 592 to 599 nm). In the case of Fano dip, it only shifts from 643 to 640 nm.

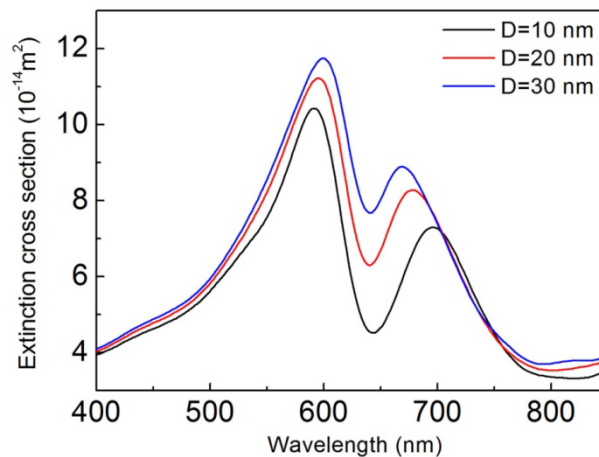


**Figure 3.** Extinction spectra of Al-Au nanorod dimers with gap distances  $d = 10, 20$  and  $30$  nm, respectively. The lengths of Al and Au nanorods are  $187$  and  $250$  nm, respectively, and the diameter of each rod is  $40$  nm.

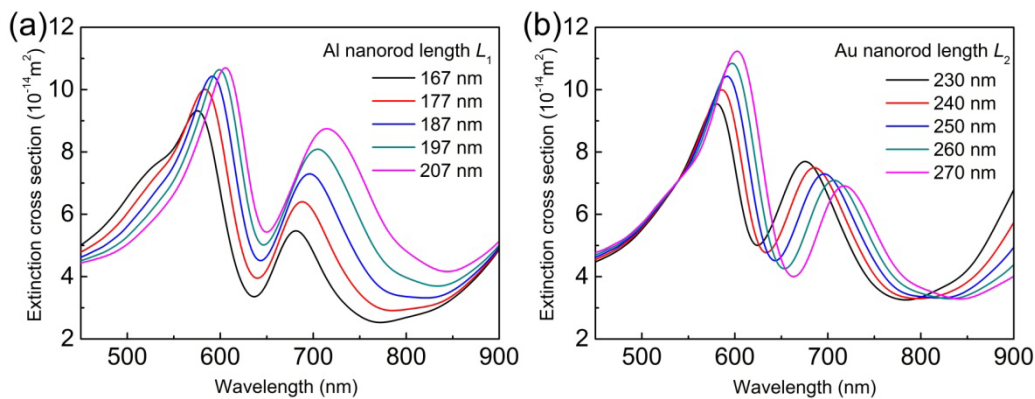


**Figure 4.** (a) Extinction spectra of Al-Au nanorod dimers with different Al nanorod length  $L_1$ , and other parameters are fixed at  $L_2 = 250$  nm and  $d = 10$  nm; (b) Extinction spectra of Al-Au nanorod dimers with different Au nanorod length  $L_2$ , and other parameters are fixed at  $L_1 = 187$  nm and  $d = 10$  nm.

The Fano resonance can also be tuned by adjusting the resonant frequencies of the bright (Al nanorod) or dark (Ag nanorod) mode, as shown in Fig. 4. In Fig. 4(a), as the bright mode wavelength redshift by increasing the length of the short Al nanorod from  $167$  to  $207$  nm with a fixed length  $250$  nm of Au nanorod, the Fano dip shows a slight redshift and becomes shallower. When the dark mode wavelength redshift by increasing the length of the long Au nanorod from  $230$  to  $270$  nm with a fixed

short Al nanorod length at 187 nm, the Fano dip still shows a red shift but becomes deeper (see Fig. 4b).

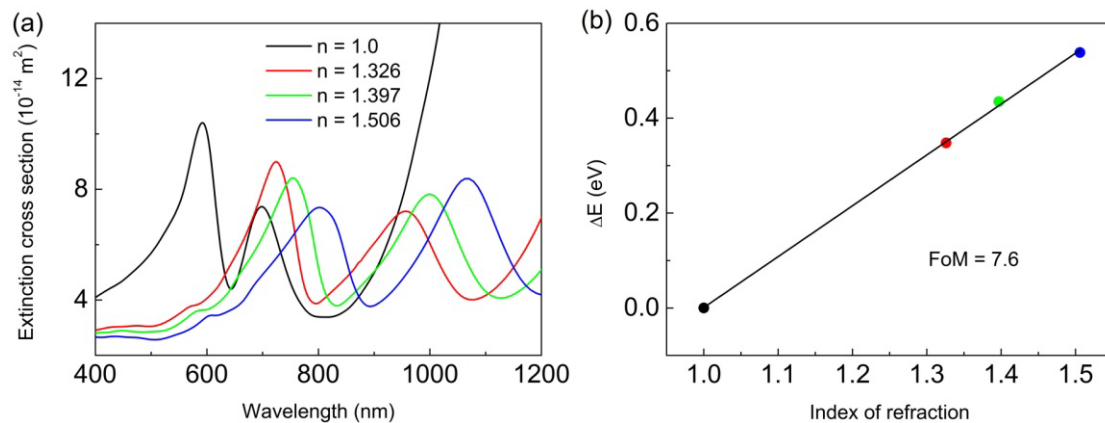


**Figure 5.** LSPR sensing in Al-Au nanorod dimer. (a) Extinction spectra of Al-Au nanorod dimer with the environment refractive index  $n$  of 1.0, 1.326, 1.397 and 1.506, respectively. (b) Linear plot of Fano dip shifts vs refractive index of the surrounding media.

One of the very interests in Fano resonance in plasmonic systems is its potential as effective localized surface plasmon resonance (LSPR) sensors, which stems from its inherent sensitivity to the surrounding environment. The efficiency of LSPR sensors is typically evaluated by their figure of merit (FoM), defined as the ratio of the plasmon energy shift per refractive index unit change in the surrounding medium, divided by the width of the spectral peak.<sup>16</sup> Here, we choose the Al-Au nanorod dimer with the same dimensional parameters as those in Fig. 2(a) to estimate its LSPR sensitivity to the refractive index change of the surrounding medium numerically. The resulting extinction spectra for the Al-Au nanorod dimer embedded in various media: ethanol ( $n = 1.326$ ), butanol ( $n = 1.397$ ) and index matching oil ( $n = 1.506$ , Cargille immersion oil) is presented in Fig. 5(a). The figure shows a pronounced redshift of the Fano resonance with the increasing surrounding refractive index. In air, the Fano resonance appears at 643 nm, and in immersion oil with a refractive index  $n = 1.506$ , it shifts to 892 nm. To determine the LSPR sensitivity, a slope of about 1.07 is obtained by a linear fit for the energy shift of the Fano dip as a function of the refractive index of the surrounding media (see Fig. 5b), and divided by the Fano line width (0.147 eV). The resulting FoM is 7.6, which is larger than those of isolated nanoparticles such as nanocubes (FoM = 5.4)<sup>29</sup> and nanoclusters (FoM = 5.7)<sup>16</sup>, and comparable with that of noncentric ring/disk nanocavity (FoM = 8)<sup>30</sup>. Comparing with homogenous plasmonic nanostructures, the obstacle in experiment is the fabrication of heterogeneous Al-Au nanorod dimers. One possible method can be realized by means of two-step electron-beam lithography and a combination of etch-down and lift-off with well-controlled spatial alignment reported in the recent work<sup>31</sup>. The proposed heterogeneous nanorod cluster may find potential application in high sensitive sensors.

#### 4. Conclusions

In this work, we investigated the hybridization of plasmonic modes between closely spaced Al-Au heterogeneous nanorod dimers arranged in a close proximity by end-to-end. Optical properties of Al-Au nanorod dimers are studied by FDTD simulation method. A pronounced Fano dip in the extinction spectra is observed, which strongly depends on both the geometry parameters of the complex nanostructure. The LSPR sensitivity of the heterogeneous metallic complex nanostructures is also checked and a FoM of 7.6 is obtained, which may find applications in biological sensing and molecule detection based on the coherent plasmonic coupling.

## Acknowledgements

This work was funded in part by the National Nature Science Fund (11104079) and the National Key Scientific Instrument Project (2012YQ150092).

## References

- [1] Atwater H A and Polman A 2010 *Nat. Mater.* **9** 205.
- [2] Lal S, Grady N K, Kundu J, Levin C S, Lassiter J B and Halas N J 2008 *Chem. Soc. Rev.* **37** 898.
- [3] Kinkhabwala A, Yu Z, Fan S, Avlasevich Y, Muellen K and Moerner W E 2009 *Nat. Photonics* **3** 654.
- [4] Wu E, Chi Y, Wu B, Xia K, Yokota Y, Ueno K, Misawa H and Zeng H 2011 *J. Lumin.* **131** 1971.
- [5] Song M, Chen G, Liu Y, Wu E, Wu B and Zeng H 2012 *Opt. Express* **20** 22290.
- [6] Song M, Wu B, Chen G, Liu Y, Ci X, Wu E and Zeng H 2014 *J. Phys. Chem. C* **118** 8514.
- [7] Wu B, Ueno K, Yokota Y, Sun K, Zeng H and Misawa H 2012 *J. Phys. Chem. Lett.* **3** 1443.
- [8] Zhong Y, Ueno K, Mori Y, Shi X, Oshikiri T, Murakoshi K, Inoue H and Misawa H 2014 *Angew. Chem. Int. Ed.* **53** 10350.
- [9] Liu N, Tang M, Hentschel M, Giessen H and Alivisatos A P 2011 *Nat. Mater.* **10** 631.
- [10] Akimov A V, Mukherjee A, Yu C L, Chang D E, Zibrov A S, Hemmer P R, Park H and Lukin M D 2009 *Nature* **450** 402.
- [11] Chi Y, Chen G, Jelezko F, Wu E and Zeng H 2011 *IEEE Photon. Technol. Lett.* **23** 374.
- [12] Chen G, Liu Y, Song M, Wu B, Wu E and Zeng H 2013 *IEEE J. Sel. Top. Quantum Electron* **19** 4602404.
- [13] Prodan E, Radloff C, Halas N J and Nordlander P 2003 *Science* **302** 419.
- [14] Fan J A, Wu C, Bao K, Bao J, Bardhan R, Halas N J, Manoharan V N, Nordlander P, Shvets G and Capasso F 2010 *Science* **328** 1135.
- [15] Jain P K, Huang W Y and El-Sayed M A 2007 *Nano Lett.* **7** 2080.
- [16] Lassiter J B, Sobhani H, Fan J A, Kundu J, Capasso F, Nordlander P and Halas N J 2010 *Nano Lett.* **10** 3184.
- [17] Ye J, Wen F, Sobhani H, Lassiter J B, Dorpe P V, Nordlander P and Halas N J 2012 *Nano Lett.* **12** 1660.
- [18] Yang Z, Hao Z, Lin H and Wang Q 2014 *Nanoscale* **6** 4985.
- [19] Cetin A E and Altug H 2012 *ACS Nano* **6** 9989.
- [20] Chen H, Shao L, Man Y, Zhao C, Wang J and Yang B 2012 *Small* **8** 1503.
- [21] Bachelier G, Russier-Antoine I, Benichou E, Jonin C, Fatti N D, Valle'e F and Brevet P 2008 *Phys. Rev. Lett.* **101** 197401.
- [22] Yang Z, Zhang Z, Zhang W, Hao Z and Wang Q 2010 *Appl. Phys. Lett.* **96** 131113.
- [23] Peña-Rodríguez O, Pal U, Campoy-Quiles M, Rodríguez-Fernández L, Garriga M and Alonso M I 2011 *J. Phys. Chem. C* **115** 6410.
- [24] Wu D, Jiang S and Liu X 2011 *J. Phys. Chem. C* **115** 23797.
- [25] Knight M W, Liu L, Wang Y, Brown L, Mukherjee S, King N S, Everitt H O, Nordlander P and Halas N J 2012 *Nano Lett.* **12** 6000.
- [26] Schwab P M, Moosmann C, Wissert M D, Schmidt E W, Ilin K S, Siegel M, Lemmer U and Eisler H 2013 *Nano Lett.* **13** 1535.
- [27] Palik E D 1985 *Handbook of Optical Constants of Solids* (Academic).
- [28] Yang Z, Zhang Z, Zhang L, Li Q, Hao Z and Wang Q 2011 *Opt. Lett.* **36** 1542.
- [29] Sherry L J, Chang S H, Schatz G C, Duyne R P V, Wiley B J and Xia Y 2005 *Nano Lett.* **101** 2034.
- [30] Hao F, Sonnefraud Y, Dorpe P V, Maier S A, Halas N J and Nordlander P 2008 *Nano Lett.* **8** 3983.
- [31] Aouani H, Rahmani M, Navarro-Cía M and Maier S A 2014 *Nat. Nanotech.* **9** 290.